Case Studies in Thermal Engineering 41 (2023) 102618

Contents lists available at ScienceDirect

Case Studies in Thermal Engineering

journal homepage: www.elsevier.com/locate/csite

Prediction of emissions and performance from transient driving cycles using stationary conditions: Study of advanced biofuels under the ETC test

Felipe Soto [a], Rubén Dorado-Vicente [b], Eloísa Torres-Jiménez [b,*], Fernando Cruz-Peragón [b]

[a] Universidade Federal de São João del-Rei, Praça Frei Orlando, 170, São João del-Rei, Minas Gerais, CEP: 36307-352, Brazil
[b] Dep. Mechanical and Mining Engineering, University of Jaén, Campus las Lagunillas, s/n, 23071, Jaén, Spain

ARTICLE INFO

Keywords:
Common-rail
Emissions prediction
Sugarcane biodiesel
Farnesane
DoE
Shape preserving parameterization

ABSTRACT

This paper applies and improves a methodology for estimating engine responses from transient cycles using steady conditions according to a Design of Experiments (DoE). The fuels tested are diesel-farnesane, biodiesel from sugarcane, and diesel fuel S50. A common-rail engine and the European Transient Cycle (ETC) are considered. Two DoEs of 13 runs each were analysed: the 13 modes of the European Stationary Cycle (ESCDoE) and a 5-level Fractional Factorial Design (FFDoE). The mathematical transformation of the engine working region and the experimental data approximation were improved using chord length parameterization and tensor product surfaces, respectively. Both DoEs provide an instantaneous approximation of engine performance responses of high accuracy. However, in general, better results are obtained using the FFDoE ($R^2 > 0.92$, but $R^2 > 0.84$ for exergy rate) compared to the ESCDoE ($R^2 > 0.87$, and $R^2 > 0.53$ for exergy rate). The FFDoE is the most appropriate design for the instantaneous prediction of THC and NOx regulated emissions ($R^2 > 0.91$) as well as for its specific (accumulated) emissions (relative error $e < 11\%$). However, worse results are obtained for CO emissions prediction ($R^2 > 0.7$ and $e < 19.1\%$).

1. Introduction

The global concern on environment has fostered governments around the world to make a remarkable effort to regulate emissions. The transportation sector seriously contributes to this problem, being the largest emitter of nitrogen oxides (NO_x) [1], in particular, diesel engines [2]. Despite the disadvantages of vehicles powered by internal combustion engines related to air pollution, the transport sector in the near future will still be powered by these types of engines [3]. The increasingly stringent regulations have accelerated the development of improved combustion technologies [4], bioblendstocks [5], new fuel additives [6], lubricating oils [7], etc. that allow for higher engine efficiency and fuel economy, showing that vehicles based on internal combustion engines are not close to their development limits.

In Europe, new vehicle emissions have been regulated through the Euro emission standards since 1992, which has led to a pollution reduction worldwide due to manufacturers find more economically viable to produce a standard low-emissions vehicle regardless of whether the destination country requires compliance with strict regulations [8]. To determine if exhaust emissions meet the limits

* Corresponding author.
E-mail address: etorres@ujaen.es (E. Torres-Jiménez).

https://doi.org/10.1016/j.csite.2022.102618
Received 7 October 2022; Received in revised form 24 November 2022; Accepted 1 December 2022
Available online 2 December 2022

imposed by the regulations, new vehicles are tested over different standardized cycles, which are defined according to the type of engine tested. The World-wide harmonized Light-Duty Vehicles Test Procedure (WLTP) is the current protocol in Europe concerning light-duty vehicles. The WLTP is based on real-driving data, while the prior procedure, the New European Driving Cycle test (NEDC) was based on theoretical driving [9]. On the other hand, heavy-duty diesel vehicles must comply with three testing protocols to ensure adherence to Euro 5 regulation: the European Stationary Cycle (ESC) and the European Transient Cycle (ETC) both for the determination of NOx, carbon monoxide (CO), hydrocarbons (HC), and particulate matter (PM), and, finally, the European Load Response test (ELR), which is a transient cycle to determine smoke opacity [10]. Currently, in Brazil, heavy-duty vehicles must comply with the Proconve P7 standard, which specifies the same three testing protocols as the Euro 5 for air pollution control. A report performed by the Brazilian association of automotive engineering [11] points out that the application of the experimental tests specified in Euro 6 is inviable in Brazil, not only because they are more complex than Euro 5 but because they require much more sophisticated equipment.

All vehicle registrations must comply with the testing protocols mentioned above, which means that a significant effort must be constantly made to decrease emissions and fuel consumption to satisfy the increasingly stringent regulations. In this sense, many researches claim the important role of biofuels, since they help to reduce gaseous emissions responsible of the greenhouse effect, mainly CO_2 emissions [12], as well as pollution rate during its burning and processing [13], for example, negligible or zero SO_x emissions [14].

Fuels such as diesel-Farnesene and sugarcane-biodiesel, which can substitute petrodiesel, are referred to as advanced biofuels due to their production involves the usage of the metabolically engineered yeast “Saccharomyces cerevisiae” which can produce both biofuels via fermentation of simple sugars [15].

The Environmental Protection Agency (EPA) has highlighted the benefits of Sugarcane-biodiesel, such as an 85% decrease in carbon footprint and the lack of sulfur, benzene, and heavy metals, compared with petrodiesel [16]. A previous study showed that, during the transient cycle ETC, neat sugarcane-biodiesel produced significantly lower NOx and PM specific emissions than diesel fuel [17]. Marques et al. obtained similar results in the same medium-duty engine [18]. Nevertheless, they noted that neat sugarcane-biodiesel remarkably reduces engine power. For this reason, they proposed the usage of a 20% (v/v) blend in regular diesel fuel since it offers similar power to neat mineral diesel fuel but with a substantial pollutant emissions reduction, mainly in NOx, PM, and smoke opacity. Similar results were obtained in the study [19], in which the authors related the behavior of PM emissions from biodiesel with the activation energy. It is important to highlight that the raw material used to produce biodiesel influences its composition and properties, as Bukkarapu and Krishnasamy [20] observed when analyzing biodiesel obtained from sugarcane instead of from an oilseed. However, atypical biodiesel, such as the one obtained from sugarcane, behaves like any other biodiesel, providing similar engine performance and emissions.

Diesel-farnesane is an isoparaffin obtained via the hydrogenation of diesel-farnesene [21]. Soriano et al. [22] experimentally tested diesel-farnesane at several stationary operating modes representative of the NEDC and found similar engine performance compared to regular diesel fuel but with significant pollutant emission reductions. Millo et al. [23] performed a study using a 30% v/v of farnesane in mineral diesel fuel to estimate emissions from the NEDC. They observed a considerable decrease in CO and HC specific emissions for the blend containing farnesane. Soto et al. [17] tested neat diesel-farnesane under the ETC testing procedure and noted lower NOx and PM specific emissions than regular diesel fuel. On the other hand, previous authors [24] inferred that farnesane offers better combustion characteristics than biodiesel.

In any case, the engine, fuel, and operating conditions tested, among others, influence emissions [25]. For example, fuel density influences the amount of fuel sprayed in volume [26]. In this sense, the amount of injected fuel increases with the increment of biodiesel in diesel fuel since the density and viscosity of the blend increase [27]. Consequently, the experimental determination of engine responses is always required to enhance engine performance and emissions, as well as to determine compliance with the regulations.

The determination of a set of stationary operating regimes that reproduces a transient standardized test cycle has an important advantage; stationary tests are less demanding than transient tests in terms of costs and the complexity of monitoring systems required. Samuel et al. [28] predicted fuel economy and emissions from a gasoline car. They concluded that a modelling approach built through a set of stationary operating regimes could be used for simulating real-world drive cycles. Other authors have tested some steady-state operating regimes with the target of simulating a transient cycle, such as Belgiorno et al. [29] and Shamun et al. [30], who chose 8 stationary points as the most representative operating points of the urban driving cycle belonging to the NEDC to determine responses from a light-duty compression ignition engine, as well as García et al. [31] who tested and simulated 3 steady-state operating conditions representative of the NEDC driving cycle. On the other hand, Pablo Fernández-Yánez et al. [32] tested several fuels in the same vehicle under stationary and transient operation. These experimental tests allowed quantifying the weight of each stationary regime during an actual driving route and separating the transient effects from the steady-state results, thus offering a wide database to develop advanced mathematical methods to model and optimize costs and time in the adjustment process of the large number of parameters involved.

Summarizing, all vehicle registrations must comply with a testing protocol for the measurement of pollutant emissions. The testing protocol applied depends on the type of engine (light or heavy). Most of these protocols are transient cycles and regulations are increasingly stringent in limiting emissions from these procedures. On the other hand, advanced biofuels can help to reach these pollutant emissions limits. The present methodology for estimating engine responses from a standardized transient cycle employing few steady-state operating conditions would decrease the complexity and requirements demanded by the experimental set-up. The big difference in the test equipment is that stationary tests, for example the ESC cycle, can be conducted operating an eddy current dynamometer. This device is more straightforward and less expensive than the dynamometers employed in non-stationary tests, such as the ETC test, which must have the “dynamic” function. In any case, these predictions can help in the process of optimizing a new

Table 1
Characteristics of the heavy-duty engine tested.

Engine Model	MAN D0834 LF05
Operation	Diesel, 4-stroke, 2 turbochargers, 2 intercoolers
Cylinders	4 in line
Displacement	4.58 L
Bore/Stroke	108 mm/125 mm
Compression ratio	16.5:1
Max power (2400 min^{-1})	166 kW
Max Torque (1100 - 1600 min^{-1})	850 Nm
Fuel Injection System	Electronic Common Rail
Standard Compliance	Euro 5

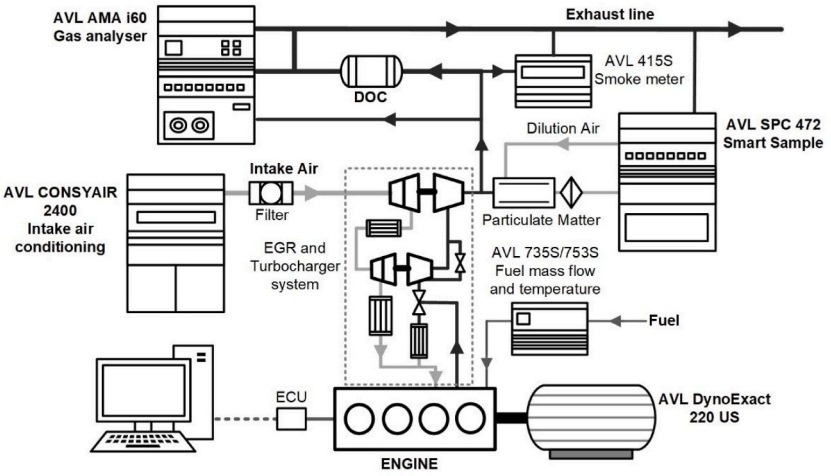

Fig. 1. Schematic representation of the test bench.

Table 2
Equipment characteristics.

Equipment		Parameter	Range [units]	Accuracy
AVL 735S/753S		Fuel mass flow Fuel supply temperature	0 ÷ 125 [kg/h] −10 ÷ 40 [°C]	±0.12%
ABB Sensy flow FMT700-P		Air flow ratio	1:40	±2% air mass
AVL Intake air conditioning CONSYSAIR 2400		Temperature Pressure Moisture	−40 ÷ +60 [°C] −400 ÷ 200 [mbar] 4 ÷ 34 [g H_20/kg dry air]	±0.5 [°C] ±1 [mbar]
Vaisala HMT333		Intake air temperature Intake air humidity	−40 ÷ +60 [°C] 0 ÷ 90%/90% ÷ 100%	±0.2 [°C] ±2%/± 3%
AVL DynoExact 220 US (Active dynamometer)		Torque Speed Power	0 ÷ 934 [Nm] 0 ÷ 10000 [rpm] 0 ÷ 220 [kW]	±0.1%
AVL Emissions test bench AMA i60	FID: Flame Ionization Detector	Total hydrocarbon (THC) CH_4	THC: 10 ÷ 20000 [ppm] CH_4: 30 ÷ 20000 [ppm]	±0.5%
	CLD: Chemilumines-cence Detector	NO, NO_X	3 ÷ 1000 [ppm]	±0.5%
	IRD: Infrared Detector	CO, CO_2	CO: 50 ÷ 5000 [ppm] CO_2: 0.1 ÷ 6 vol%	±0.5%
	PMD: Paramagnetic Detector	O_2	0 ÷ 25%	±0.5%
	QCL: Quantum Cascade Laser	N_2O	±0.5%	5 ÷ 1000 [ppm]

engine for its compliance with the regulations since this procedure can be used as a calibration methodology [33].

A methodology to determine a Design of Experiments (DoE) that predicts vehicle performance and emissions during a transient test, where each point of the design represents a stationary mode, was explained in a previous paper [34]. This paper revealed that, for the

Table 3
Properties of the tested fuels.

Property	Unit	Diesel S50	Sugarcane diesel-farnesane	Sugarcane biodiesel
Approximate summarized formula	[−]	$C_{15.2}H_{27.3}$[a]	$C_{15}H_{32}$	$C_{16}H_{30}O_2$
H/C		1.796	2.133	1.875
Cetane number	[−]	49.0	58.7	69.9
Density at 20 °C	kg L^{-1}	0.843	0.770	0.875
Viscosity at 40 °C	mm^2 s^{-1}	3.110	2.710	3.326
Lower heating value (LHV)	MJ kg^{-1}	42.03	43.43	35.80
	MJ L^{-1}	35.43	33.44	31.32
Stoichiometric air-fuel ratio $(A/F)_{st}$	[−]	14.50	14.98	12.23
$LHV/(A/F)_{st}$	MJ kg_{air}^{-1}	2.899	2.899	2.927
Distillation 10% vol	°C	196.0	250.5	280.0
Distillation 50% vol	°C	260.0	252.0	294.0
Distillation 90% vol	°C	340.0	254.0	306.0

[a] the oxygen was not considered due to its low mass fraction.

validation case studied (the NEDC and diesel fuel), main cumulative and instantaneous performance responses could be accurately predicted using a DoE built with a few stationary points, as well as the cumulative response concerning regulated exhaust emissions. Nevertheless, the instantaneous values of exhaust emissions deviate significantly from the actual values, which is in concordance with the study of Liu et al. [35], who observed notable differences in instantaneous emissions, especially at low loads, from a spark ignition engine following the NEDC compared to stationary regimes.

The fuel, testing cycle, vehicle, or engine do not influence the proposed approximation approach based on a mathematical transformation of the engine-working domain into a square domain. The target of the present paper is to apply this methodology to a different engine, transient cycle and fuel, supporting the feasibility of the methodology. In this case, the experimental data come from testing a medium duty engine following the ETC procedure and powered by advanced biofuels (sugarcane diesel-farnesane and sugarcane biodiesel). An additional target of the present study is to improve the algorithm used for the mapping procedure and the polynomial surfaces that approximate the experimental data.

2. Materials and methods

2.1. Experimental set-up

Experimental responses from the ETC test are used to validate the methodology. The ETC test is part of the current Brazilian regulation concerning heavy-duty engines. The available experimental set-up provides engine performance and emissions responses. Table 1 shows the engine's main characteristics. Fig. 1 depicts the test bench used to determine stationary and transient engine responses, and Table 2 provides some relevant data regarding the testing devices whose data are used in the present work. Gaseous emissions are evaluated after the Diesel Oxidation Catalyst (DOC). A previous paper [17] analyses the engine responses obtained during the ETC procedure. These data are used in the present work to validate the methodology applied.

Besides the experimental data obtained, Eqs. (1) and (2) [36] are used to calculate the exhaust gas residual heat rate ($\dot{Q}_{eg}$) and its thermomechanical exergy rate ($\dot{E}_{eg}$):(1)

$$\dot{Q}_{eg} = \dot{m}_{eg}\left(h_{eg} - h_0\right), \tag{1}$$

$$\dot{E}_{eg} = \dot{m}_{eg}\left[h_{eg} - h_0 - T_0\left(s_{eg} - s_0\right)\right], \tag{2}$$

Where $\dot{m}$ refers to mass flow, T to temperature, h to specific enthalpy, s to specific entropy, the subscript eg to exhaust gas, the 0 to the ambient condition. $\dot{m}_{eg}$ is calculated by adding the intake air $\dot{m}_a$ and fuel mass flow rate $\dot{m}_f$.

2.2. Tested fuels

Parameters regarding engine performance and emissions from three fuels are used for the validation of the methodology applied. These fuels are diesel S50, which contains 5% biodiesel and is sold at gas stations in Brazil, sugarcane biodiesel, and diesel-farnesane. The most important properties of these fuels are shown in Table 3.

2.3. Description of the improved methodology for testing standardized engine cycles

Standardized transient tests, such as the ETC, NEDC, or WLTP, specify vehicle speed versus time. Engine responses are experimentally determined during the cycle. The conventional testing procedure can be performed in two ways; the first uses a roller test bench where the whole vehicle is tested, and its speed is modified by varying the resistance of the roller. In the second one, just the engine is tested at those operating regimes calculated based on the longitudinal dynamic equations [36,37] applied to the particular vehicle that carries the tested engine. These equations provide the torque and engine speed (controllable input variables, also called factors) versus time.

Nowadays, the engine calibration stage is critical in the development process of a vehicle. This calibration must face the increasingly stringent emissions limits for different standardized cycles and the high complexity of the engine control strategies among

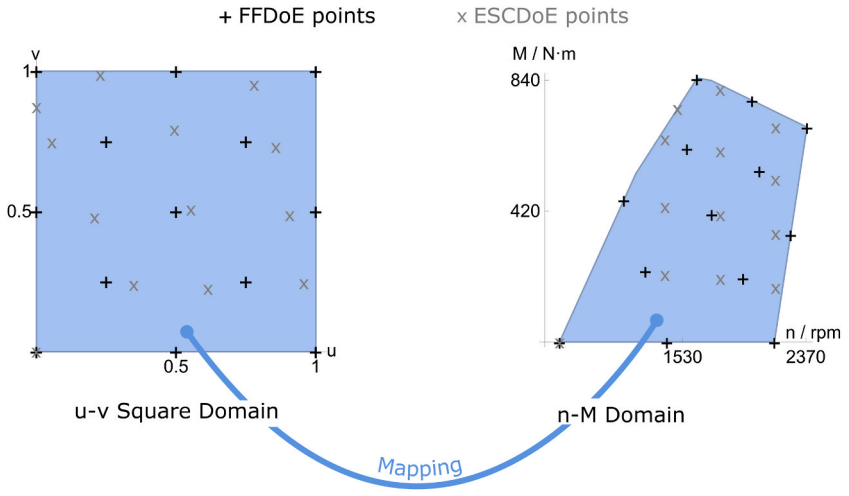

Fig. 2. FFDoE and ESCDoE points distributions in the *u-v* unit-square domain and their corresponding positions in the *n-M* domain.

others. In these cases, efficient methods and tools become essential to reduce costs and time in the tuning process of the large number of parameters involved. Advanced mathematical methods for modeling and optimizing have been developed to solve this problem. Castagné et al. [33] describe several calibration methods to optimize the NEDC based on DoE. According to that study, the genuine local approach is one of the most common processes for calibrating engines; 17 operating points were selected to represent the overall driving cycle. The choice of these points is not an easy task since it is necessary to determine the contribution of each operating point to the whole cycle. The methodology presented here solves this problem.

The fact that the *n-M* domain is, in general, a free-form 2D region hinders a selection of the stationary set of points independently of the testing cycle, fuel and engine, and building simple surface approximations. According to Torres-Jiménez et al. [34], this problem can be overcome by mapping the *n-M* domain into a *u-v* square domain. The results showed that it is possible to predict instantaneously and cumulatively the main engine performance responses of a transient cycle, as well as the cumulative predicted emissions response, using steady-state operating modes according to a DoE of 13 runs.

In the present paper, the methodology proposed in Ref. [34] is tested to determine if it is applicable to any transient cycle, fuel, or engine. Additionally, the original transformation of the engine-working domain is improved by the definition of a chord length parameterization, while a polynomial surface approximates the experimental data. Finally, the methodology is validated for a different engine (a medium-duty one), cycle (the ETC cycle), and fuels (diesel-farnesane, biodiesel from sugarcane, and diesel S50) than those analysed in Ref. [34]. The following Subsections summarize the methodology.

2.3.1. *Mapping between n-M and unit-square domains*

To get a polynomial approximation, the straightforward choice for the domain is the unit square. On the other hand, according to Floater [38], to get a shape-preserving parameterization, a good placement of the boundary points is by chord length. Following the chord-length parameterization described by Farin [39], the *n-M* boundary points $\mathbf{d}_i$ are mapped to $\mathbf{u}_i$ on the unit square. The points on the square depend on the distance between boundary points $L_i = |d_{i+1} - d_i|$:

$$\boldsymbol{u}_{i+1} = u_i + \mu \cdot L_i$$

where $\mu = 4/L$ and L is the boundary length. Note that the product $\mu \cdot L_i$ provides the proportional distance between points scaled by 4, which is the total length of the square boundary. Therefore, the above equation provides the places of the di points along the boundary length.

The $\mathbf{u}_i$ points are triangulated to get the triangulation *T*, which is applied to the *u-v* and the *n-M* domains. Every point **p** in the triangulation *T* is within a triangle *j*, so that it can be defined as a linear combination of its vertices $\mathbf{v}_{k,j}$, k = {1, 2, 3}:

$$p = \sum_{k=1}^{3} b_k \cdot v_{k,j}, \sum_{k=1}^{3} b_k = 1,$$

where **b** are the barycentric coordinates [39].

The barycentric coordinates are the same in the unit-square and the *n-M* domain, which allows the mapping *F* between both domains. Let **p** be a point in one domain with a triangulation *T*, then the mapping *F*(**p**, *T*, **b**) provides a point **P** within another domain with the same triangulation.

2.3.2. *Experimental results approximation*

Two DoE's of 13 points each are analysed, the responses measured are mapped into the unit-square by means of *F*, and fitted to low degree (lower than the number of DoE points) tensor product polynomial surfaces (those that are built by the interpolation of a set of

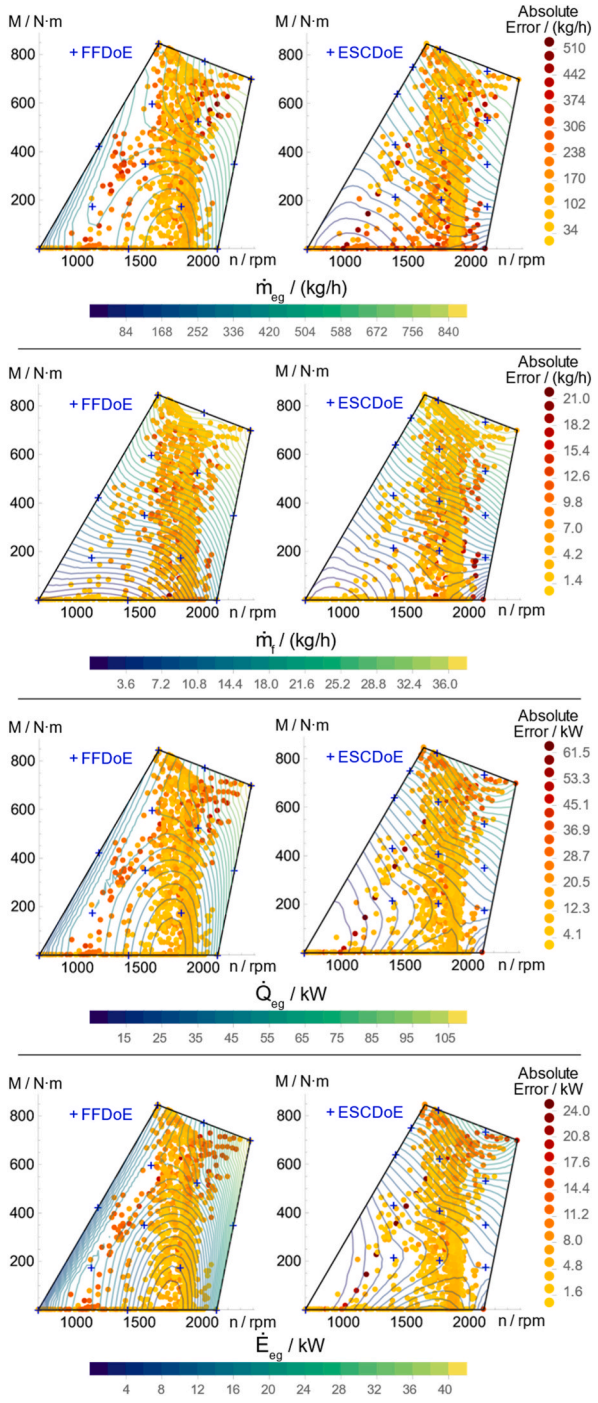

Fig. 3. Approximated responses ($\dot{m}_{eg}$, $\dot{m}_f$ (kg/h), $\dot{Q}_{eg}$ (kW), and $\dot{E}_{eg}$ (kW)) in the *n-M* domain for **diesel S50** using the two DoEs analysed (FFDoE and ESCDoE) and contour plot of the absolute error.

parametric polynomial curves) [39] using the least mean square method, which allow an independent control of the polynomial approximation degree in the *u-v* directions. The polynomial surface degree used in this work is the lowest one that leads to the highest R^2 and requires fewer coefficients than the number of DoE points. The mapping F allows changing between the surface in the unit-square and the surface in the general domain.

2.3.3. Experimental designs studied

To assess the application of the above method, the ETC responses of a heavy-duty engine fueled by 3 different fuels: diesel S50,

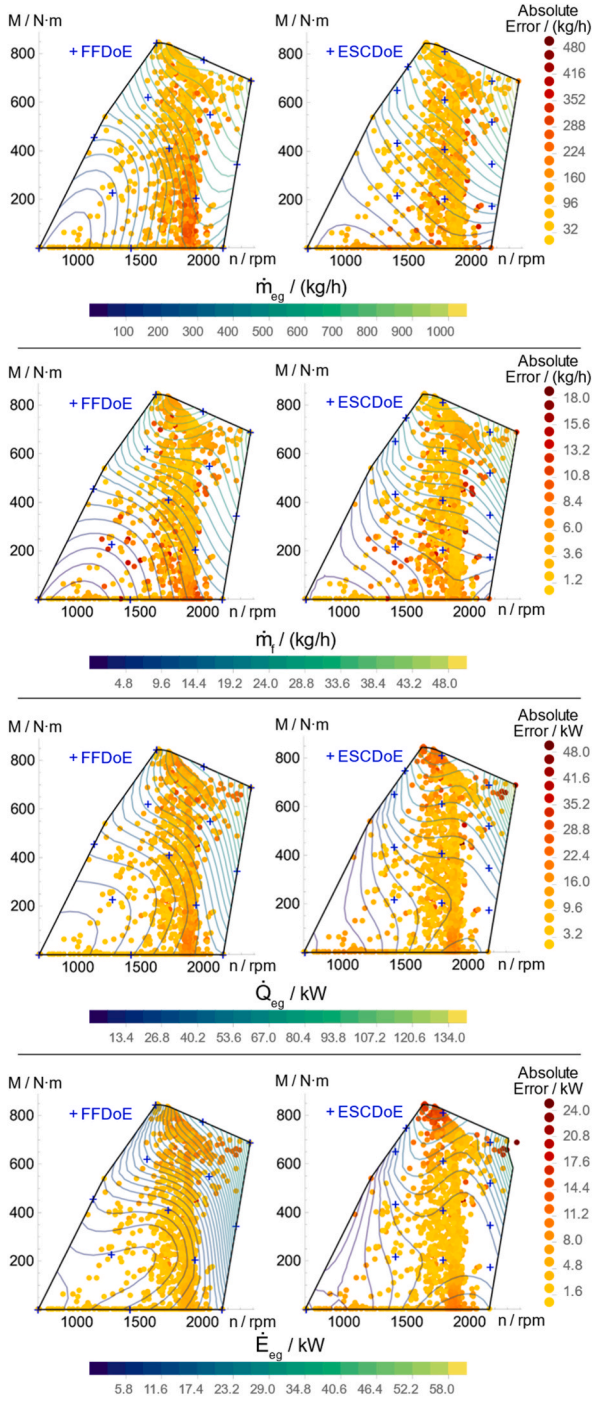

Fig. 4. Approximated responses ($\dot{m}_{eg}$, $\dot{m}_f$ (kg/h), $\dot{Q}_{eg}$ (kW), and $\dot{E}_{eg}$ (kW)) in the *n-M* domain for **diesel-farnesane** using the two DoEs analysed (FFDoE and ESCDoE) and contour plot of the absolute error.

diesel-farnesane, and sugarcane biodiesel, are approximated using 13 stationary operating regimes placed in the *n-M* domain in 2 different ways.

Fig. 2 shows the stationary points distribution in the *u-v* unit-square and their corresponding positions in the *n-M* domain. Torres-Jiménez et al. [34] and Cruz-Peragón et al. [40] claim that the best distribution for a set of 13 stationary modes is a fractional factorial design of five levels (FFDoE), which suitably meets optimality criteria, while the ESC distribution (ESCDoE) corresponds with the 13 modes of the European Stationary Cycle (ESC).

For the tested fuels, the authors have the experimental ESC and the ETC data, whose results have already been published [17,41].

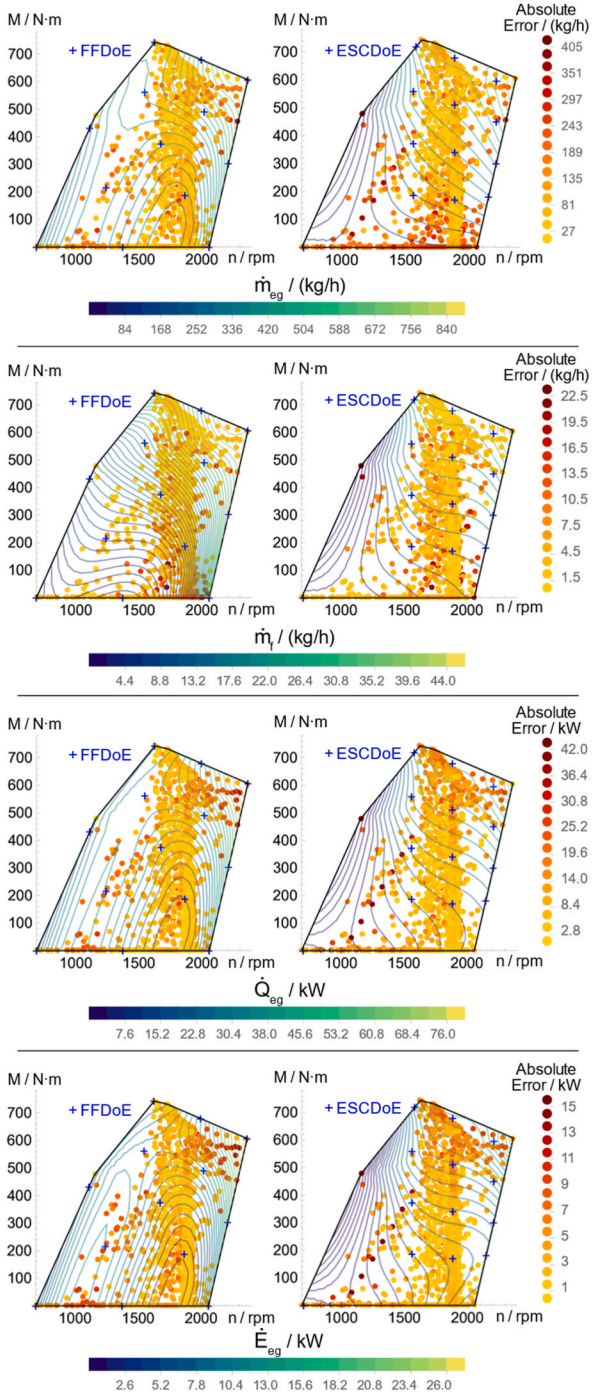

Fig. 5. Approximated responses ($\dot{m}_{eg}$, $\dot{m}_f$ (kg/h), $\dot{Q}_{eg}$ (kW), and $\dot{E}_{eg}$ (kW)) in the *n-M* domain for **sugarcane biodiesel** using the two DoEs analysed (FFDoE and ESCDoE) and contour plot of the absolute error.

To assess the approximation method, the ESCDoE was accomplished using the actual information. Nevertheless, for the FFDoE, the stationary responses are estimated at the corresponding distribution points using a linear interpolation of the ETC measurements: those corresponding to stationary states.

2.3.4. Validation results

The polynomial surface $S(n, M)$ estimates a specific ETC response with respect to each (n, M) point. In this case, the following responses are estimated: $\dot{Q}_{eg}$, $\dot{E}_{eg}$, $\dot{m}_{eg}$, $\dot{m}_f$, and the standardized THC, NOx and, CO emissions. On the other hand, it is possible to rebuild

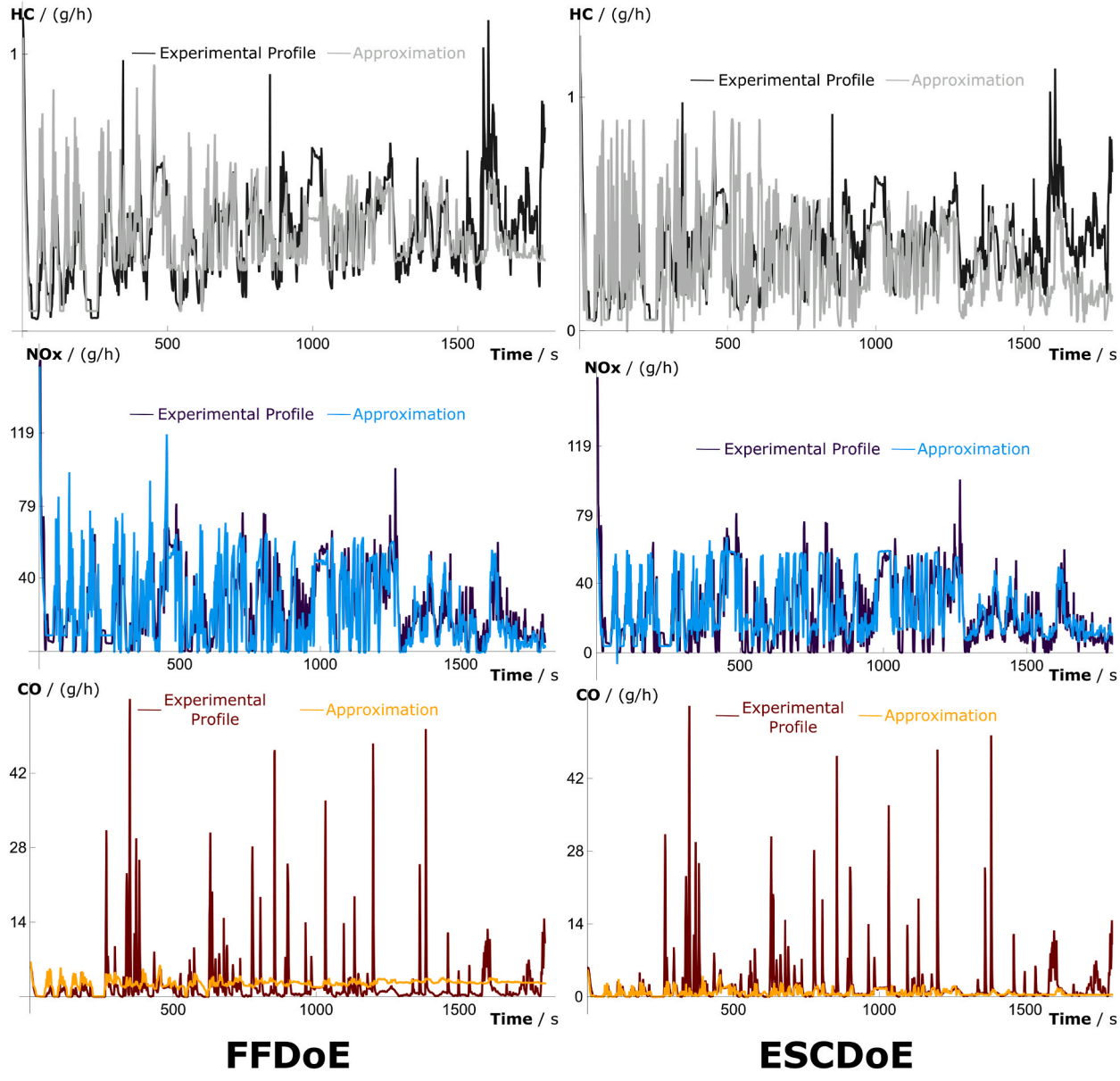

Fig. 6. Experimental and approximated instantaneous emission profiles (**HC** (g/h), **NO$_x$** (g/h), **CO** (g/h)) for diesel S50 using the two DoEs analysed (FFDoE and ESCDoE).

the ETC for a specific response: the response values along the time $R(t)$, just following the sequence of test points (n, M) defined by the ETC test procedure [10]. From the estimated cycle responses, we can compute the specific emissions as it is explained in the Brazilian standard [42] and in the European Directive 1999/96/EC [10].

A set of metrics helps to evaluate the agreement between the approximations and the experimental ETC data. Regarding $\dot{m}_{eg}$, $\dot{m}_f$, $\dot{Q}_{eg}$, and $\dot{E}_{eg}$, the absolute error and the determination coefficient R^2 between the actual data and S were determined. Besides, the relative error e and R^2 were the metrics used to compare actual and estimated THC, NO_x, and CO specific (accumulated) emissions. The coefficient of determination R^2 helps to assess the goodness of the fit. For the computation of that metric, the predicted values are the FFDoE or ESCDoE estimations for the 1800 ETC speed-torque data. The measurement system provides data every 0.1 s despite the ETC standard specifying a sampling rate of 1 s. Therefore, to accommodate the experimental data to the standard, the 1800 points along the cycle (1 measurement every 1 s) have been taken from a linear regression of the total experimental data measured (18000 points: 1 point every 0.1 s).

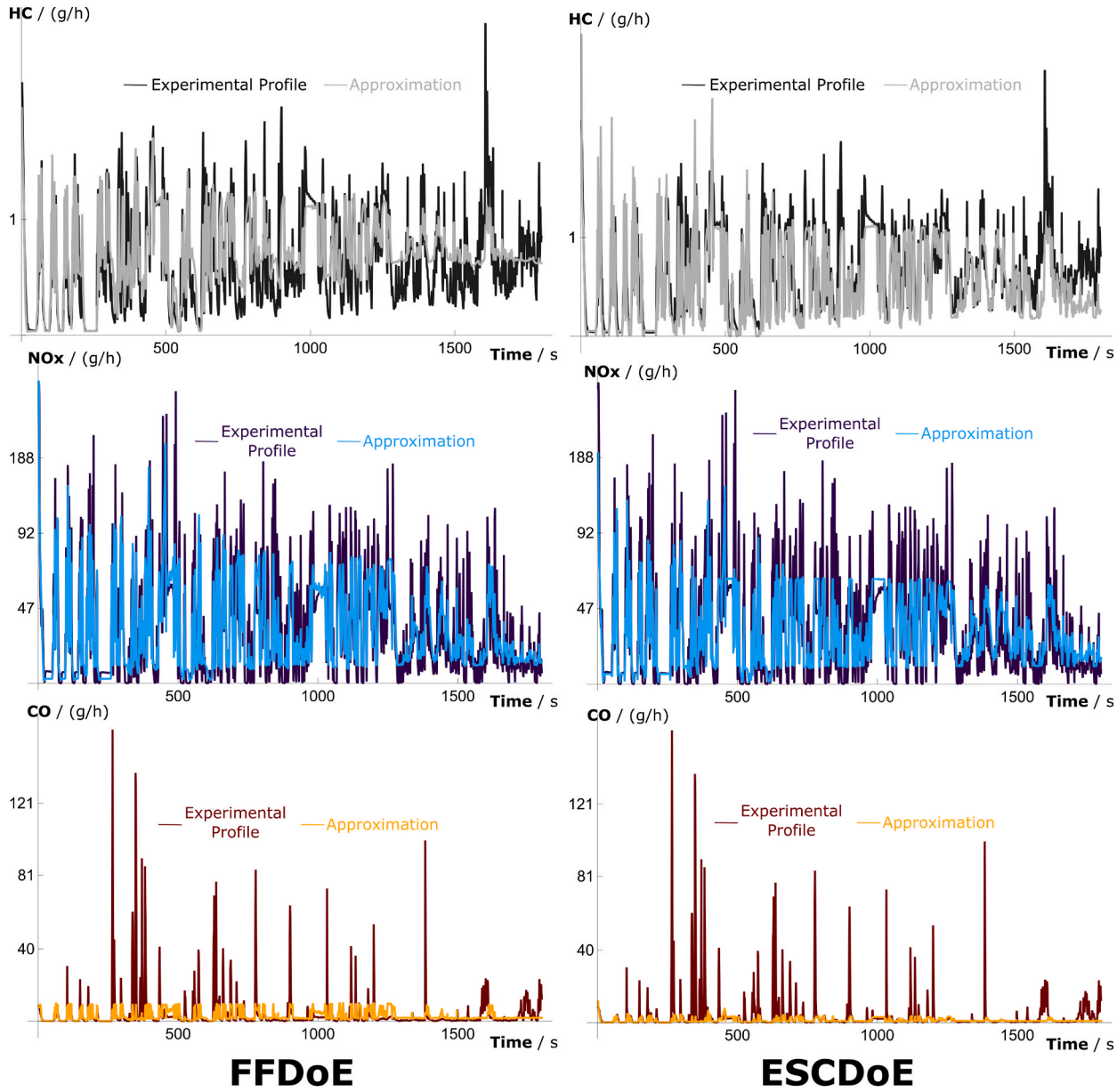

Fig. 7. Experimental and approximated instantaneous emission profile (**HC** (g/h), **NO$_x$** (g/h), **CO** (g/h)) for **diesel-farnesane** using the two DoEs analysed (FFDoE and ESCDoE).

3. Results and discussion

Next Figures show the approximated responses for the three fuels tested using the two DoEs analysed. Fig. 3, Fig. 4, and Fig. 5 portray the contour plot of the absolute error of the following engine responses in the *n-M* domain: $\dot{m}_{eg}$ (kg/h), $\dot{m}_f$ (kg/h), $\dot{Q}_{eg}$ (kW), and $\dot{E}_{eg}$ (kW), while Fig. 6, Fig. 7, and Fig. 8 show the experimental and approximated instantaneous profiles during the ETC cycle of the following emissions: THC (g/h), NO_x (g/h), and CO (g/h). Figs. 3, Fig. 4, and Fig. 5 illustrate engine responses and the high accuracy of the prediction obtained via the FFDoE and the ESCDoE for all tested fuels. On the other hand, in Figs. 6, Fig. 7, and Fig. 8, it can be observed that both designs of experiments provide profiles whose tendency is in good agreement with the instantaneous experimental ones, except for the case of CO emissions. Note the high variability at specific times in the CO profile; most likely, for this reason, it is hard to fit the instantaneous response by means of a low-degree polynomial approximation.

Table 4 shows the value of the metric R^2 defined in Section 2.3.4 for each fuel tested. This metric is used to evaluate the agreement between experimental and estimated responses. It is observed that, in general, for performance responses ($\dot{m}_{eg}$, $\dot{m}_f$, $\dot{Q}_{eg}$, and $\dot{E}_{eg}$), the FFDoE design provides similar or better instantaneous results ($R^2 > 0.92$) compared to the ESCDoE ($R^2 > 0.87$), except for $\dot{E}_{eg}$ whose

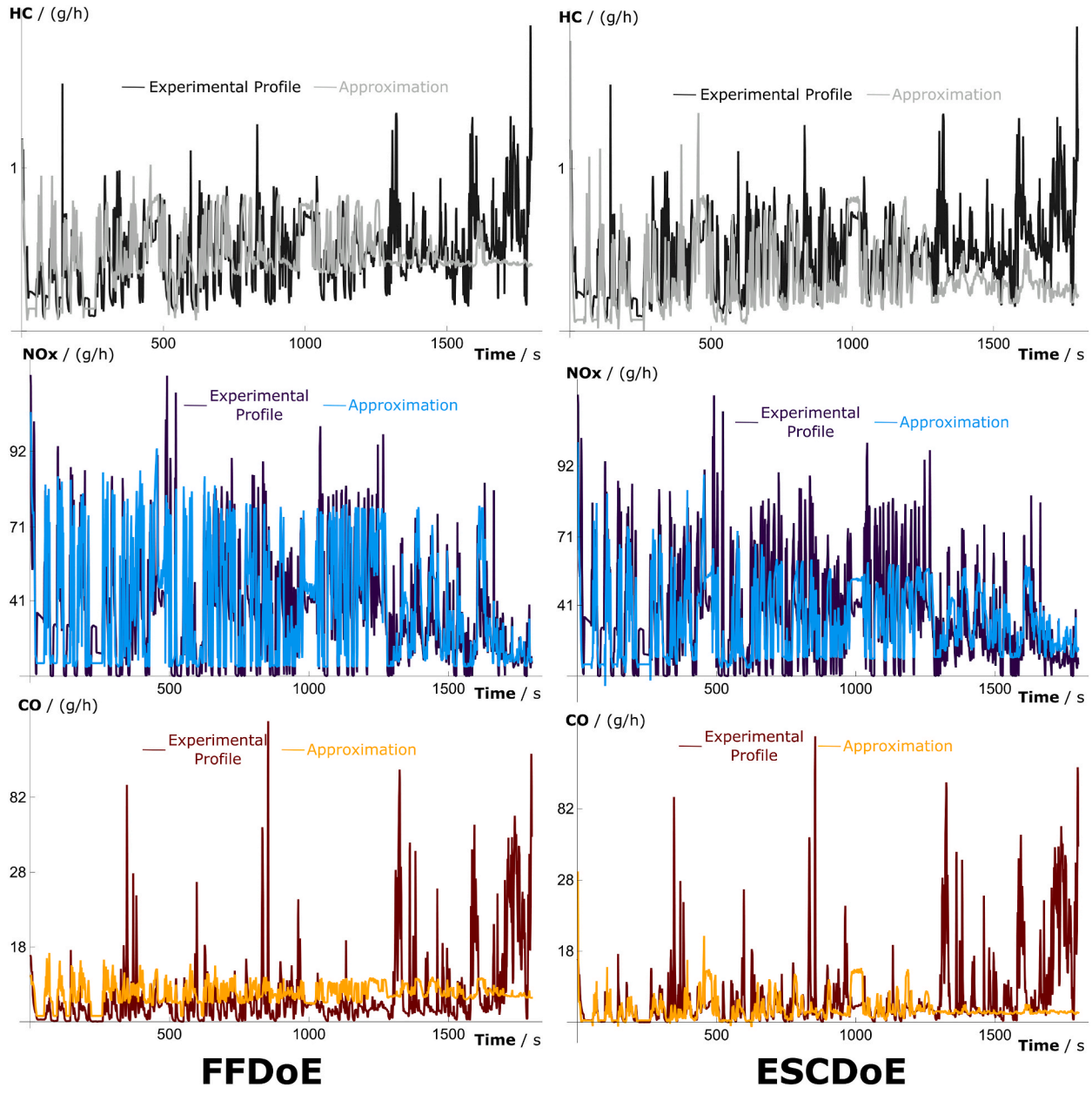

Fig. 8. Experimental and approximated instantaneous emission profile (**HC** (g/h), **NO$_x$** (g/h), **CO** (g/h)) for sugarcane biodiesel using the two DoEs analysed (FFDoE and ESCDoE).

Table 4
Measurement of the agreement real/estimated responses via R^2 considering the two DoEs analysed and the three fuels tested.

Response	Diesel S50		Sugarcane diesel-farnesane		Sugarcane biodiesel	
	FFDoE	ESCDoE	FFDoE	ESCDoE	FFDoE	ESCDoE
$\dot{m}_{eg}$	0.97	0.94	0.92	0.98	0.98	0.88
$\dot{m}_f$	0.97	0.98	0.93	0.96	0.93	0.98
$\dot{Q}_{eg}$	0.93	0.94	0.93	0.91	0.94	0.87
$\dot{E}_{eg}$	0.86	0.88	0.87	0.53	0.84	0.80
THC	0.94	0.73	0.95	0.95	0.93	0.88
NOx	0.91	0.88	0.92	0.87	0.92	0.70
CO	0.76	0.42	0.70	0.47	0.77	0.58

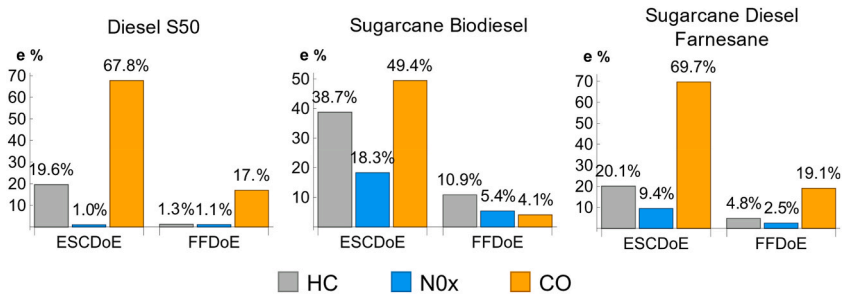

Fig. 9. Relative errors *e* for the approximated specific emissions (**HC** (g/kW·h), **NO_x** (g/kW·h), **CO** (g/kW·h)) for the three fuels tested using the two DoEs analysed (FFDoE and ESCDoE).

agreement is good enough for the FFDoE ($R^2 > 0.84$) but unacceptable for the ESCDoE ($R^2 > 0.53$). Regarding emissions, again, the most recommended design for determining THC and NO_x is the FFDoE ($R^2 > 0.91$), and the same is noted for CO emissions, but R^2 is lower ($R^2 > 0.7$) although remarkably higher than those obtained via the ESCDoE ($R^2 > 0.42$).

Finally, Fig. 9 shows the relative errors obtained when approximating the specific emissions regulated by the ETC standard (HC, NOx, and CO) for the three fuels tested and considering the ESCDoE and FFDoE designs. In general, and comparing both designs of experiments, the FFDoE provides better results than the ESCDoE for all the fuels tested. The FFDoE can approximate HC, NOx, and CO specific emissions with a relative error below 11%, 6%, and 20%, respectively. All emissions from sugarcane biodiesel can be approximated via the FFDoE with a relative error below 11%, while it provides the highest error (19.1%) for sugarcane diesel-farnesane CO specific emissions. It is interesting to highlight the low relative errors for diesel S50 when approximating HC and NOx emissions, 1.3% and 1.1% respectively, when using the FFDoE. Note that NOx and HC experimental profiles of S50 fuel show lower oscillations than those obtained for the biofuels (see Figs. 6, Fig. 7, and Fig. 8). This fact leads to a remarkably better fitting using low-degree polynomials, which explains the low relative error for S50 observed in Fig. 9.

4. Conclusions

In this paper, the feasibility of a methodology previously developed by the authors for estimating engine responses of a transient cycle from 13 stationary modes is corroborated for two advanced biofuels (diesel-farnesane and sugarcane biodiesel) powering a medium duty engine, and considering the ETC cycle. Two DoEs of 13 points are analysed: the FFDoE (a fractional factorial design of five levels) and the experimental points defined in the European Stationary Cycle (ESCDoE).

Two improvements to the methodology are included consisting, firstly, on a new way of performing the mapping of the working region by the definition of a chord length parameterization, which is shape-preserving, besides, the resulting mapping computation is straightforward if both domains have the same triangulation (linear combinations of the corresponding triangles vertices). Secondly, polynomial surfaces performed via a tensor product are used to approximate the experimental data, which allow an independent control of the polynomial approximation degree in the *u*-*v* directions.

From the obtained results, it can be concluded that the prediction of instantaneous engine responses, such as $\dot{Q}_{eg}$, $\dot{m}_{eg}$, and $\dot{m}_f$, is of high accuracy using both DoEs, although, in general, better results are obtained using the FFDoE ($R^2 > 0.92$), which supports the conclusions of previous studies. The same design is recommended for the instantaneous and specific emissions prediction of THC, and NOx ($R^2 > 0.91$ and $e < 11\%$). However, worse results are obtained for of CO emissions prediction ($R^2 > 0.7$ and $e < 19.1\%$) due to the high variability at specific times in the CO experimental profiles.

CRediT authorship contribution statement

Felipe Soto: Conceptualization, Validation, Investigation, Resources, Supervision, Project administration, Funding acquisition. **Rubén Dorado-Vicente:** Conceptualization, Methodology, Software, Validation, Formal analysis, Resources, Data Curation, Writing - Original Draft, Visualization. **Eloísa Torres-Jiménez:** Conceptualization, Methodology, Formal analysis, Resources, Data Curation, Writing - Original Draft, Writing - Review & Editing. **Fernando Cruz-Peragón:** Conceptualization, Methodology, Validation, Formal analysis, Supervision, Project administration, Funding acquisition.

Declaration of competing interest

The authors declare that they have no known competing financial interests or personal relationships that could have appeared to influence the work reported in this paper.

Data availability

Data will be made available on request.

Acknowledgments

Eloísa Torres-Jiménez is grateful for the Research Mobility Grant from the Spanish Ministry of Science, Innovation, and Universities (José Castillejo CAS19/00245). In addition, the authors thank the same Ministry for the financial support obtained through Project RECUPERA-TE (RTI2018-095923-B-C21). This work was also supported by MAN-Latin America, which funded the engine experimental tests performed at MAHLE Metal Leve S.A., the acquisition of the biofuels from the companies Amyris and LS9 in Brazil, and made the engine available for the experimental tests with all the necessary accessories and technical support.

References

[1] Y. Van Fan, S. Perry, J.J. Klemeš, C.T. Lee, A review on air emissions assessment: Transportation, J. Clean. Prod. 194 (2018) 673–684.
[2] R. Pillai, V. Triantopoulos, A.S. Berahas, M. Brusstar, R. Sun, T. Nevius, et al., Modeling and predicting heavy-duty vehicle engine-out and tailpipe nitrogen oxide (NOx) emissions using deep learning, Front. Mech. Eng. (2022) 11.
[3] L. Lešnik, B. Kegl, E. Torres-Jiménez, F. Cruz-Peragón, Why we should invest further in the development of internal combustion engines for road applications, Oil & Gas Sci. Technol. Rev. d'IFP Energ. nouvelles 75 (2020) 56.
[4] C. Berggren, T. Magnusson, Reducing automotive emission - the potentials of combustion engine technologies and the power of policy, Energy Pol. 41 (2012) 636–643.
[5] V.L. Dagle, M. Affandy, J.S. Lopez, L. Cosimbescu, D.J. Gaspar, S.S. Goldsborough, et al., Production, fuel properties and combustion testing of an iso-olefins blendstock for modern vehicles, Fuel 310 (2022), 122314.
[6] T. Kegl, A.K. Kralj, B. Kegl, M. Kegl, Nanomaterials as fuel additives in diesel engines: a review of current state, opportunities, and challenges, Prog. Energy Combust. Sci. 83 (2021), 100897.
[7] B. Tormos, J.M. García-Oliver, M. Carreres, C. Moreno-Montagud, B. Domínguez, M.D. Cárdenas, et al., Experimental assessment of ignition characteristics of lubricating oil sprays related to low-speed pre-ignition (LSPI), Int. J. Engine Res. (2021), 14680874211013268.
[8] M. Crippa, G. Janssens-Maenhout, D. Guizzardi, S. Galmarini, EU effect: exporting emission standards for vehicles through the global market economy, J. Environ. Manag. 183 (2016) 959–971.
[9] T. Donateo, M. Giovinazzi, Building a cycle for real driving emissions, Energy Proc. 126 (2017) 891–898.
[10] EU, Directive 1999/96/EC of the European Parliament and of the Council of 13 December 1999 on the approximation of the laws of the Member States relating to measures to be taken against the emission of gaseous and particulate pollutants from compression ignition engines for use in vehicles, and the emission of gaseous pollutants from positive ignition engines fuelled with natural gas or liquefied petroleum gas for use in vehicles and amending Council Directive 88/77/EEC, Off. J. Eur. Union OJ L 44 (2000) 1–155.
[11] A.E.A. Comissão Técnica de Pesados da, Euro VI Análise do Programa Europeu, impactos e desafios para a realidade brasileira, AEA – Associação Brasileira de Engenharia Automotiva, 2016, pp. 1–49. DT AEA 002/15.
[12] V.V. Shahare, B. Kumar, P. Singh, Biofuels for sustainable development: a global perspective, in: Green Technologies and Environmental Sustainability, Springer, 2017, pp. 67–89.
[13] R.A. Mattioda, D.R. Tavares, J.L. Casela, O.C. Junior, Social life cycle assessment of biofuel production, in: J. Ren, A. Scipioni, A. Manzardo, H. Liang (Eds.), Biofuels for a More Sustainable Future, Elsevier, 2020, pp. 255–271.
[14] R. Ruan, Y. Zhang, P. Chen, S. Liu, L. Fan, N. Zhou, et al., Chapter 1 - biofuels: introduction, in: A. Pandey, C. Larroche, C. Dussap, E. Gnansounou, S.K. Khanal, S. Ricke (Eds.), Biofuels: Alternative Feedstocks and Conversion Processes for the Production of Liquid and Gaseous Biofuels, second ed., Academic Press, 2019, pp. 3–43.
[15] N.A. Buijs, V. Siewers, J. Nielsen, Advanced biofuel production by the yeast Saccharomyces cerevisiae, Curr. Opin. Chem. Biol. 17 (2013) 480–488.
[16] https://www.epa.gov/greenchemistry/presidential-green-chemistry-challenge-2010-small-business-award. (Accessed 14 February 2022).
[17] F. Soto, G. Marques, E. Torres-Jiménez, B. Vieira, A. Lacerda, O. Armas, et al., A comparative study of performance and regulated emissions in a medium-duty diesel engine fueled with sugarcane diesel-farnesane and sugarcane biodiesel-LS9, Energy 176 (2019) 392–409.
[18] G. Marques, L. Izquierdo, C. Coutinho, A Comprehensive Evaluation of Performance and Emissions from UltraClean™ Diesel in Medium Duty Engines, 2014. SAE Technical Paper 2014-01-2766.
[19] F. Soto, M. Alves, J.C. Valdés, O. Armas, P. Crnkovic, G. Rodrigues, et al., The determination of the activation energy of diesel and biodiesel fuels and the analysis of engine performance and soot emissions, Fuel Process. Technol. 174 (2018) 69–77.
[20] K.R. Bukkarapu, A. Krishnasamy, Predicting engine fuel properties of biodiesel and biodiesel-diesel blends using spectroscopy based approach, Fuel Process. Technol. 230 (2022), 107227.
[21] S. Guilherme, in: Amyris (Ed.), Manual do Diesel de Cana, 2012.
[22] J.A. Soriano, R. García-Contreras, D. Leiva-Candia, F. Soto, Influence on performance and emissions of an automotive diesel engine fueled with biodiesel and paraffinic fuels: GTL and biojet fuel farnesane, Energy Fuel. 32 (2018) 5125–5133.
[23] F. Millo, S. Bensaid, D. Fino, S.J. Castillo Marcano, T. Vlachos, B.K. Debnath, Influence on the performance and emissions of an automotive Euro 5 diesel engine fueled with F30 from Farnesane, Fuel 138 (2014) 134–142.
[24] C.C. Conconi, P.M. Crnkovic, Thermal behavior of renewable diesel from sugar cane, biodiesel, fossil diesel and their blends, Fuel Process. Technol. 114 (2013) 6–11.
[25] M. Lapuerta, O. Armas, J. Rodríguez-Fernández, Effect of biodiesel fuels on diesel engine emissions, Prog. Energy Combust. Sci. 34 (2008) 198–223.
[26] R. Behçet, Performance and emission study of waste anchovy fish biodiesel in a diesel engine, Fuel Process. Technol. 92 (2011) 1187–1194.
[27] E. Öztürk, Performance, emissions, combustion and injection characteristics of a diesel engine fuelled with canola oil–hazelnut soapstock biodiesel mixture, Fuel Process. Technol. 129 (2015) 183–191.
[28] S. Samuel, D. Morrey, M. Fowkes, D. Taylor, C. Garner, L. Austin, Numerical Investigation of Real-World Gasoline Car Drive-Cycle Fuel Economy and Emissions, 2004. SAE Technical Paper 2004-01-0635.
[29] G. Belgiorno, G. Di Blasio, S. Shamun, C. Beatrice, P. Tunestål, M. Tunér, Performance and emissions of diesel-gasoline-ethanol blends in a light duty compression ignition engine, Fuel 217 (2018) 78–90.
[30] S. Shamun, G. Belgiorno, G. Di Blasio, C. Beatrice, M. Tunér, P. Tunestål, Performance and emissions of diesel-biodiesel-ethanol blends in a light duty compression ignition engine, Appl. Therm. Eng. 145 (2018) 444–452.
[31] A. García, J. Monsalve-Serrano, B. Heuser, M. Jakob, F. Kremer, S. Pischinger, Influence of fuel properties on fundamental spray characteristics and soot emissions using different tailor-made fuels from biomass, Energy Convers. Manag. 108 (2016) 243–254.
[32] P. Fernández-Yáñez, J.A. Soriano, F. Soto, O. Armas, B. Pla, V. Bermúdez, Pollutant emissions from Euro 6 light duty vehicle tested under steady state and transient operation on a roller test bench with hydrogenated paraffinic and biodiesel fuels, Fuel 323 (2022), 124173.
[33] M. Castagné, Y. Bentolila, F. Chaudoye, A. Hallé, F. Nicolas, D. Sinoquet, Comparison of engine calibration methods based on design of experiments (DoE), Oil Gas Sci. Technol. Rev de l'IFP. 63 (2008) 563–582.
[34] E. Torres-Jiménez, O. Armas, L. Lešnik, F. Cruz-Peragón, Methodology to simulate normalized testing cycles for engines and vehicles via design of experiments with low number of runs, Energy Convers. Manag. 177 (2018) 817–832.
[35] Q. Liu, J. Fu, G. Zhu, Q. Li, J. Liu, X. Duan, et al., Comparative study on thermodynamics, combustion and emissions of turbocharged gasoline direct injection (GDI) engine under NEDC and steady-state conditions, Energy Convers. Manag. 169 (2018) 111–123.
[36] Y. Cengel, M.A. Boles, Thermodynamics: an Engineering Approach, fourth ed., SI Units, 2002.

[37] T.D. Gillespie, Fundamentals of vehicle dynamics, SAE International, 2021, pp. 1–400. ISBN 9781468601770.
[38] M.S. Floater, Parametrization and smooth approximation of surface triangulations, Comput. Aided Geomet. Des. 14 (1997) 231–250.
[39] G.E. Farin, G. Farin, Curves and Surfaces for CAGD: a Practical Guide, Morgan Kaufmann, 2002.
[40] F. Cruz-Peragón, E. Torres-Jiménez, L. Lešnik, O. Armas, Methodology improvements to simulate performance and emissions of engine transient cycles from stationary operating modes: a case study applied to biofuels, Fuel 312 (2022), 122977.
[41] F. Soto, G. Marques, L. Soto-Izquierdo, E. Torres-Jiménez, S. Quaglia, F. Guerrero-Villar, et al., Performance and regulated emissions of a medium-duty diesel engine fueled with biofuels from sugarcane over the European steady cycle (ESC), Fuel 292 (2021), 120326.
[42] ABNT, Road Vehicles — Analysis and Evaluation of Exhaust Gas According to ETC, ESC and ELR Cycles. Brazilian Association of Technical Standards, NBR 15634 Standard, 2012. Brazil.